Chiral-racemic phase diagrams of blue-phase liquid crystals

D. K. Yang and P. P. Crooker
Department of Physics and Astronomy, University of Hawaii, Honolulu, Hawaii 96822
(Received 5 January 1987)

We have measured the phase diagrams of mixtures of chiral and racemic CE4, CE5, and CE2 in order to study the effect of varying chirality on the existence of blue phases in chiral liquid crystals. We observe three blue phases—BPI, BPII, and BPIII—which progressively appear at the isotropic phase boundary as the chirality is increased. The temperature widths of both BPI and BPIII become wider with increasing chirality, while BPII becomes narrower and vanishes at high chirality. We argue that this may be a universal feature of blue-phase temperature-chirality phase diagrams and discuss our results in light of previous theory and experiment.

I. INTRODUCTION

The cholesteric blue-phase liquid-crystal system provides a way of studying how chirality affects the thermodynamic properties of a material.[1-3] When a nematic phase, which is not chiral, is heated, it transforms directly to the isotropic phase. If the nematic is somehow made chiral, new phases appear between the lower phase (now called cholesteric) and the isotropic phase. These new phases are the blue phases. Experimentally, three distinct blue phases have been found—BPI and BPII, which are thought to have body-centered-cubic and simple-cubic symmetry, respectively, and BPIII, which is apparently amorphous.

A theory for this behavior has been constructed by Hornreich and Shtrikman[2,4] (HS) who have studied the affect of adding a chiral term to the Landau–de Gennes free energy[5] of the nematic phase. With the addition of the chiral term, the locally nematic director acquires a spatial rotation about an axis perpendicular to itself and a new characteristic length, the pitch P for one director rotation, is established. The *chirality* of this structure is defined as the quantity $1/P$ which appears as the coefficient of the chiral term. When the pitch is long and the chirality is small, the usual cholesteric phase condenses out of the isotropic phase. When the pitch is short and the chirality is large, phases with various cubic symmetries become energetically preferable near the cholesteric-isotropic transition temperature. These new phases are representative of the blue phases. From the HS theory, Grebel, Hornreich, and Shtrikman[6] (GHS) have derived a number of phase diagrams in which phase-transition temperatures are plotted versus chirality, with chirality treated as an independent thermodynamic parameter. In these diagrams, the various blue phases appear at different chiralities, their temperature widths increasing monotonically with increasing chirality.

An important feature of the GHS phase diagrams, which should be tested experimentally, is the possibility that there are universal features associated with the appearance of the blue phases. In the theory, a variation of the chirality alone causes the appearance of the blue phases. In most condensed matter systems, making such an independent variation of chirality *experimentally* is not easily achieved. In liquid-crystal systems, however, chirality *can* be varied independently—either by mixing left- and right-handed versions of the same chiral material, or equivalently, by mixing a chiral material with its racemate. To good approximation, the resulting mixtures will vary only in chirality—that is, only in the size of the chiral Landau coefficient. The other Landau coefficients will remain essentially unchanged since, except for chirality, the two components are chemically identical.

Phase diagrams of chiral-racemic mixtures have been reported previously,[7-9] however, so far they have failed to show any universal features. For the material of Marcus and Goodby[7] (MG), BPI existed only over a short range of chirality, giving way to only BPII and BPIII at high chiralities. For the compound CE6 (see Table I), reported by Tanimoto *et al.*[8] and Collings,[9] the width of BPII tended to become narrower at high chiralities while both BPI and BPIII widths were still increasing in temperature width.

Here we report new chiral-racemic phase diagrams for the compounds CE4, CE5, and CE2 (see Table I). These diagrams are compared with those for CE6 and the MG material. We also have measured the chirality of these

TABLE I. Structures of CE4, CE5, CE6, and CE2.

BDH[a] name	n	Structure[b]
CE4	6	$C_nH_{2n+1}OPhCO\cdot OPhCH_2\overset{*}{C}H(CH_3)CH_2CH_3$
CE5	8	
CE6	10	
CE2		$CH_3CH_2\overset{*}{C}H(CH_3)CH_2PhPhCO\cdot OPhCH_2\overset{*}{C}H(CH_3)CH_2CH_3$

[a]British Drug House.
[b]Ph = 1, 4 substituted phenyl ring.

compounds as a function of chiral concentration and we report on the selective reflection wavelengths observed. Our main conclusion is that BPII *disappears with increasing chirality.* This may be a universal feature of blue phases and we attempt to reconcile this fact with the diagrams of CE6 and the MG material. A secondary observation is the presence of forbidden selective reflections, reported in another material by Tanimoto and Crooker[10] and as yet unexplained.

II. MATERIALS

The chiral liquid crystals CE4, CE5, and CE2 and their racemates CE4R, CE5R, and CE2R were obtained from British Drug House and used as received. CE4, CE5, and CE6 are three members of a homologous series containing chiral alkyl and achiral alkoxy endchains; they differ only in the length of their alkoxy endchains[11] CE2 is structurally different—it has two chiral alkyl endchains and is correspondingly more chiral than the CE4–6 series.[11] The "racemic" CE2 supplied to us is not actually a true racemate: If the handedness of each endchain is given by *S* or *R*, then equal proportions of (SS), (SR), (RS), and (RR) are present. Our racemic CE2 thus consists of two pairs of enantiomers—(SS)/(RR) and (SR)/(RS).

III. EXPERIMENT

Chiral-racemic mixtures for each system were constructed in approximately 50-mg quantities with chiral concentrations having a relative precision of 0.2%. Measurements were first made of the pitch *P*, which was determined at a temperature less than 1 °C below the cholesteric phase boundary. For CE4, CE5, and CE6, the method used was to place the sample between a convex lens and a flat microscope slide, both of whose surfaces had been treated for parallel alignment by rubbing with cotton. When the cholesteric phase is viewed between crossed linear polarizers by reflected light, a characteristic colored Cano ring pattern is observed. This pattern is well understood;[12] from the measured ring radii and the known lens radius, the pitch can be readily calculated. For CE2, the high temperatures involved ($\simeq$120 °C) made it difficult to use the lens method for every chiral concentration. Consequently, we measured both the pitch (via the lens method) and the selective reflection wavelength $\lambda = 530$ nm at a 30% chiral concentration, from which the refractive index $n = 1.68$ was calculated using the relation $\lambda = nP$. We then measured selective reflection wavelengths for the remaining chiral concentrations and converted the values to pitches using the same refractive index. Any systematic error introduced by dispersion of the refractive index we estimate to be less than 3%.

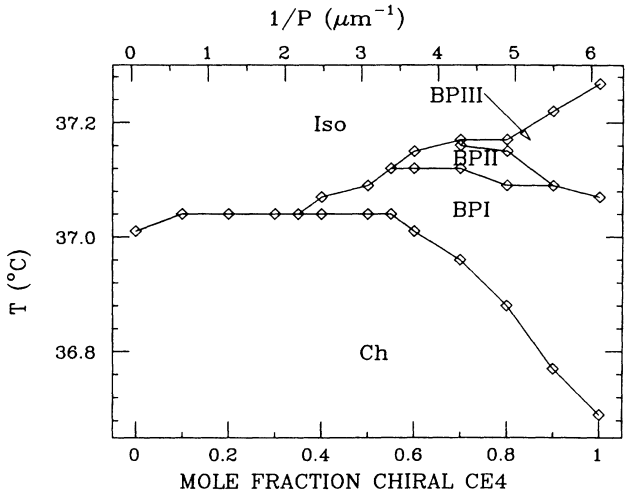

FIG. 2. Phase diagram showing transition temperatures vs mole fraction chiral material for CE4. The chirality scale is derived from Fig. 1.

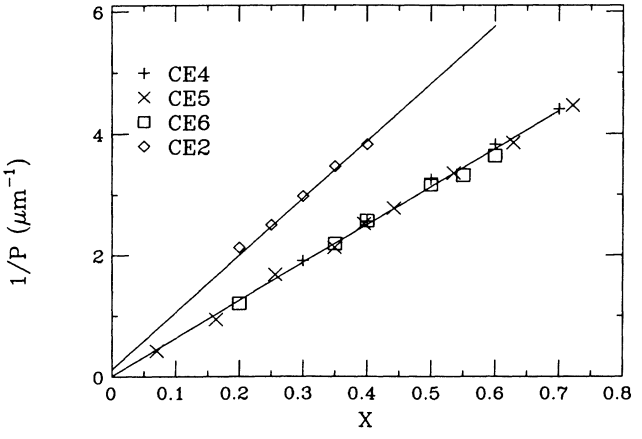

FIG. 1. Chirality $1/P$ vs chiral concentration X for CE4, CE5, CE6, and CE2. The lines are best linear fits to the data, with CE4–6 taken as one data set.

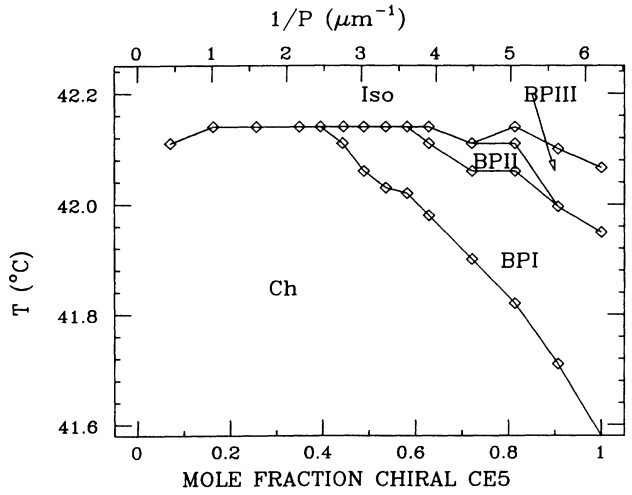

FIG. 3. Phase diagram for CE5.

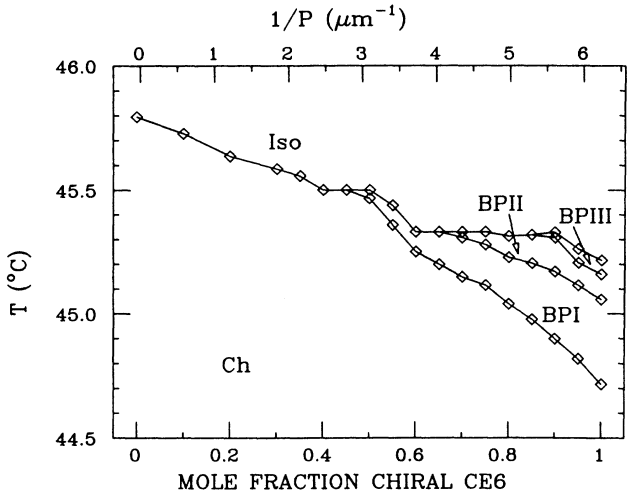

FIG. 4. Phase diagram for CE6. Data are taken from Refs. 8 and 9.

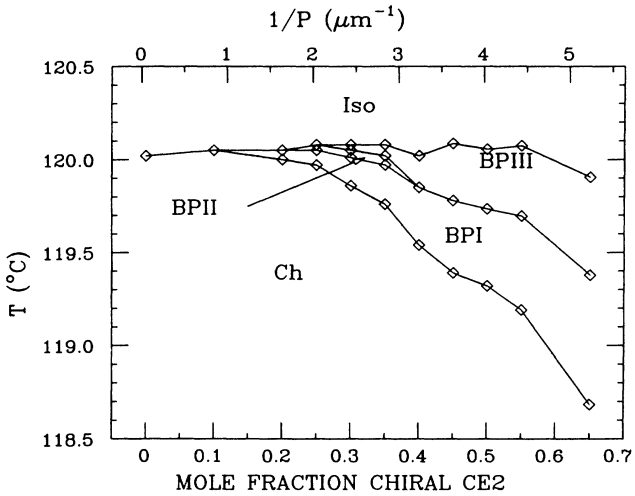

FIG. 5. Phase diagram for CE2.

Figure 1 shows the chirality $1/P$ plotted for each material as a function of X, the mole fraction of chiral material in the chiral-racemic mixture. Racemic CE5 turned out to be slightly chiral; assuming that it was a mixture of one CE5 enantiomer and true racemate, we corrected the measured chiral concentrations to show the actual amount of chiral CE5 in Fig. 1. Within experimental error the chiralities increase linearly with X. Furthermore, the chiralities of CE4, CE5, and CE6 all have the same concentration dependence, while CE2 is approximately 50% more chiral for any concentration.

We next measured phase diagrams for each material. For low chiral concentrations where the pitch is relatively long, the selective reflection wavelengths and blue-phase textures are visually observable by reflection microscopy so that the transition temperatures can be directly determined. At higher chiral concentrations, however, the selective reflection wavelengths move into the ultraviolet region, making detection by reflected light impossible. The transition temperatures can nevertheless still be determined using transmitted light microscopy. For the isotropic BPIII transition, the higher rotary power of BPIII can be distinguished from that of the isotropic phase by slightly rotating the analyzer about the crossed position. Dispersion in the BPIII rotatory power[13] will cause the sample to appear blue for a rotation in one direction and yellow for the other, unlike the situation in the isotropic phase where rotating the analyzer does not produce different colors. To detect the other BP transitions, transmitted light is still sufficient to faintly see the various textures and determine the transition temperatures, as long as the selective reflection wavelengths are not too short. With such a technique we were able to determine the phase diagram of CE4, CE5, and CE6 to the completely chiral limit, while that of CE2 could only be determined to a concentration of 65% chiral material.

The phase diagrams are displayed in Figs. 2—5. Note that since we have previously established the linear depen-

TABLE II. Observed selection wavelengths for CE2.

x	nP	No. 1	No. 2	No. 3	No. 4	Disallowed symmetries
			BPI			
0.4	443	611	440			$T^4O^1O^5O^6O^7$
0.35	500	661	479			
0.30	573		554			O^5
0.25	678		677	564	481	sc O^5
			BPII			
0.4	443	in uv region				
0.35	500	544				$T^4O^1O^6O^7$
0.30	573	634	461			$T^4O^1O^5O^6O^7$
0.25	676	765	550	454		$T^4O^1O^5O^6O^7$ sc

dence of chirality on chiral concentration, we are able to plot the chirality at the top of each diagram.

Finally, we spectroscopically obtained the selective reflection wavelengths for the cholesteric, BPI, and BPII phases of each system. These reflections are useful for showing the allowed symmetries of a phase; here we report only the data for CE2 (Table II).

IV. DISCUSSION

From the data shown in Fig. 1, it can be seen that the cholesteric pitch varies linearly with chiral concentration X for all our materials. This linear behavior is due to the nearly identical structure of the component right- and left-handed molecules; much more complex behavior is not unusual in mixtures of *unlike* right- and left-handed molecules.[14] Since the goal of mixing chiral materials with their racemates is to alter the chirality alone in a simple fashion, we feel the observed linear dependence justifies the technique. We let this linear variation of pitch P be given by $P=P_0/X$, where P_0 is the pitch of the pure chiral material. For CE4, CE5, and CE6, a linear fit to all the data taken at once yields $P_0=0.16$ μm, while for CE2, $P_0=0.10$ μm.

For all of our materials, BPI appears at the lowest chirality, followed by BPII and BPIII at higher chiralities. In the CE4–6 series (Figs. 2–4), the lowest chirality at which the blue phases commence increases as the length of the alkoxy chain increases, from CE4 ($1/P>2.2$ μm^{-1}), to CE5 ($1/P>2.5 \mu m^{-1}$), and to CE6 ($1/P>2.8$ μm^{-1}). CE2 (Fig. 5) is significantly different from the other materials, however, in that the blue phases commence at a lower minimum chirality ($1/P>1.5$ μm^{-1}) than in the CE4–6 series. This fact, coupled with the higher intrinsic chirality of CE2, leads to a much greater range of blue-phase chiral concentrations in CE2 ($X>25\%$) than in the CE4–6 series ($X>40\%$).

The relatively small variations between the CE4–6 phase diagrams are presumably caused by correspondingly small differences in the coefficients of the nonchiral terms in the Landau–de Gennes free energy, which are in turn due to the differing lengths of the alkoxy endchains. In CE2, both the core structure and the endchains are different from the CE4–6 molecules, which affects both the chiral and achiral coefficients. From an experimental point of view, the longer-pitch blue phases of CE2 make it a better candidate for visually observing the blue phases over a large chirality range.

The most significant feature of our phase diagrams is that at high chiralities, the temperature widths of BPI and BPIII become larger while that of BPII becomes narrower and eventually vanishes entirely. In fact, BPII is already unstable at $X=0.35$ in CE2 where it is only observable by heating. This termination of BPII is clearly seen in our CE2, CE4, and CE5 mixtures but not in CE6. Corresponding behavior has also been reported in the CE2–$\overline{7}$S5 phase diagram of Miller *et al.*[15] In fact, of all the chiral-racemic blue-phase diagrams exhibited to date, only CE6 (Refs. 8 and 9) and the MG material[7] do not show a limited BPII range. In the case of CE6, BPII narrows but does not vanish at the highest achievable chirality. From the trends qualitatively evident in the phase diagrams as they progress from CE4 to CE6, we argue that the whole CE6 phase diagram has been shifted to higher chiral concentration, so that a chirality sufficient to show the termination of BPII is not realized even for pure chiral CE6. For the MG material, a possible explanation can be achieved by the removal of *one* connecting line (no alteration of the data points) in the MG phase diagram. The new diagram would then have BPII rather than BPI terminating at high chirality and would appear very similar to ours.[16]

Our experimental phase diagrams are significantly different from the theoretically derived diagrams of GHS.[6] In the first place, all of the *experimental* phase diagrams show the blue phases first appearing, with increasing chirality, at the boundary of the isotropic phase. The *theoretical* GHS diagram also show blue phases appearing at the isotropic boundary; but, in addition, BP phases originate at the cholesteric boundary, contrary to experimental results to date. Secondly, the termination of BPII with increasing chirality has not been observed in any of the theoretically derived phase diagrams of GHS. Since this feature is found in the materials reported here, it should be theoretically explainable. Thus we believe that more theoretical work is necessary.

Finally, we comment on the measurement of selective reflection wavelengths in CE2 (Table II). It has been proposed that BPI has a chiral body-center-cubic (bcc) structure, while BPII is chiral simple cubic (sc). For each of these broad designations, a number of allowed space groups are possible, each exhibiting certain disallowed selective reflections for specific light polarizations according to general symmetry principles.[17] For a number of materials, BPI is believed to have bcc $O^8(I4_132)$ space-group symmetry, while BPII is believed to have sc $O^2(P4_232)$ symmetry.[18] In Table II the selective reflections are reported for back reflections (180° scattering) using a crossed linear polarizer and analyzer. The selective reflections for BPI are all consistent with O^8 symmetry, but the observation of the third line in BPII (this would be the sc $\langle 111 \rangle$ reflection) is forbidden and *not* consistent with any sc symmetry. Similar results have been reported by Tanimoto and Crooker[10] for another material. We emphasize that the relative intensity of the CE2 selective reflection was not weak, but was comparable in strength with other allowed reflections.

Contradicting this result and in line with the observations of others,[18] we noticed that when BPII appeared out of the BPIII phase its growth took the form of transient square platelets having the wavelength of either the sc $\langle 100 \rangle$ or the bcc $\langle 110 \rangle$ reflection. For sc $\langle 100 \rangle$, the platelet morphology is exactly that expected from crystal symmetry, while for bcc $\langle 110 \rangle$, square platelets are not consistent with the symmetry and are entirely unexpected. Thus the observed reflections and the platelet morphology lead to different conclusions. We currently have no explanation for these observations.

V. CONCLUSION

In order to study how the appearance of blue phases depends on chirality, we have presented experimental

chiral-racemic phase diagrams for several blue-phase liquid crystals. Our principle result is that BPI, BPII, and BPIII all grow out of the isotropic phase boundary at progressively increasing chirality, but that BPII vanishes at high chiralities. These results should be qualitatively explained by theoretical phase diagrams, in which chirality is also treated as an independently adjustable parameter. In fact, there are significant differences between experiment and theory, most notably the vanishing of BPII. While more experimentally derived phase diagrams are necessary, the observations so far indicate that our observed features may well be universal features of blue-phase systems in general, and, if so, they should be incorporated into existing theory.

ACKNOWLEDGMENTS

We thank B. Sturgeon of British Drug House for materials and P. J. Collings and M. Marcus for helpful discussions. This work was supported by National Science Foundation, Solid State Chemistry Grant No. DMR-8404519.

[1]P. P. Crooker, Mol. Cryst. Liq. Cryst. **98**, 31 (1983); H. Stegemeyer, Th. Blumel, K. Hiltrop, H. Onusseit, and F. Porsch, Liq. Cryst. **1**, 1 (1986).

[2]H. Grebel, R. M. Hornreich, and S. Shtrikman, Phys. Rev. A **28**, 1114 (1983).

[3]V. A. Belyakov and V. E. Dmitrienko, Usp. Fiz. Nauk **146**, 369 (1985) [Sov. Phys.—Usp. **28**, 535 (1985)].

[4]R. M. Hornreich and S. Shtrikman, J. Phys. (Paris) **41**, 335 (1980).

[5]P. G. de Gennes, Mol. Cryst. Liq. Cryst. **12**, 193 (1971).

[6]H. Grebel, R. M. Hornreich, and S. Shtrikman, Phys. Rev. A **30**, 3264 (1984).

[7]M. Marcus and J. W. Goodby, Mol. Cryst. Liq. Cryst. Lett. **72**, 297 (1982). Their material is teraphthaloyloxy-bis-4-(2′-methylbutyl) benzoate.

[8]K. Tanimoto, P. P. Crooker, and G. C. Koch, Phys. Rev. A **32**, 1893 (1985).

[9]P. J. Collings, Phys. Rev. A **33**, 2153 (1986).

[10]K. Tanimoto and P. P. Crooker, Phys. Rev. A **29**, 1566 (1984).

[11]G. W. Gray and D. G. McDonnell, Mol. Cryst. Liq. Cryst. **48**, 37 (1978).

[12]R. Cano, Bull. Soc. Fr. Mineral. Crystallogr. **91**, 20 (1968).

[13]P. J. Collings, Mol. Cryst. Liq. Cryst. **30**, 1990 (1984).

[14]J. E. Adams and W. E. L. Haas, Mol. Cryst. Liq. Cryst. **15**, 27 (1971).

[15]J. D. Miller, P. R. Battle, P. J. Collings, D. K. Yang, and P. P. Crooker, Phys. Rev. A (to be published).

[16]We thank M. Marcus for a discussion of this point.

[17]R. M. Hornreich and S. Shtrikman, Phys. Rev. A **28**, 1791 (1983).

[18]See Ref. 3 for a summary of the arguments for primitive cubic BPII.